ACS chemical biology

Letters

pubs.acs.org/acschemicalbiology

First Structure of Protein Kinase CK2 Catalytic Subunit with an Effective CK2β-Competitive Ligand

Jennifer Raaf,[†] Barbara Guerra,[‡] Ines Neundorf,[†] Bertan Bopp,[§] Olaf-Georg Issinger,[‡] Joachim Jose,[§] Markus Pietsch,[∥] and Karsten Niefind*[,†]

[†]Department für Chemie, Institut für Biochemie, Universität zu Köln, Zülpicher Straße 47, D-50674 Köln, Germany

[‡]Institut for Biokemi og Molekylær Biologi, Syddansk Universitet, Campusvej 55, DK-5230 Odense, Denmark

[§]Institut für Pharmazeutische und Medizinische Chemie, Westfälische Wilhelms-Universität Münster, PharmaCampus, Corrensstraße 48, D-48149 Münster, Germany

[∥]Institut für Pharmakologie, Universitätsklinikum Köln, Gleueler Straße 24, D-50931 Köln, Germany

Supporting Information

ABSTRACT: The constitutively active Ser/Thr kinase CK2 (casein kinase 2) is used by tumor cells to acquire apoptosis resistance. CK2 exists as a heterotetrameric holoenzyme with two catalytic chains (CK2α) attached to a dimer of noncatalytic subunits (CK2β). A druggable cavity at the CK2β interface of CK2α allows the design of small molecules disturbing the CK2α/CK2β interaction and thus affecting activity, stability, and substrate specificity. We describe here the first structure of CK2α with an effective CK2β-competitive compound, namely, a 13-meric cyclic peptide derived from the C-terminal CK2β segment. Some well-ordered water molecules not visible in CK2 holoenzyme structures were detected at the interface. Driven mainly by enthalpy, the peptide binds with submicromolar affinity to CK2α, stimulates its catalytic activity, and reduces effectively the CK2α/CK2β affinity. The results provide a thermodynamic and structural rationalization of the peptide's CK2β-competitive functionality and pave thus the way to a peptidomimetic drug addressing the CK2α/CK2β interaction.

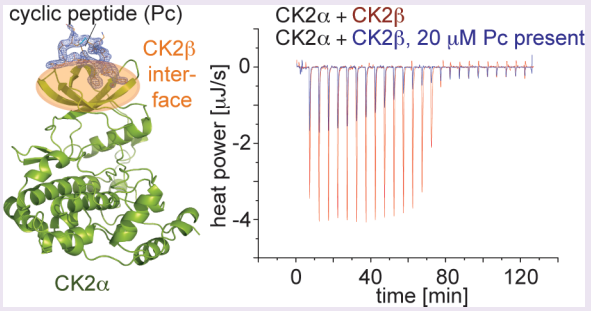

CK2 (former name, casein kinase 2) is a highly conserved Ser/Thr kinase with a heterotetrameric quaternary structure in which two catalytic subunits (CK2α) are attached to a central dimer of noncatalytic subunits (CK2β).[1] The enzyme is linked to cancer and several other human pathologies.[2] CK2 itself is no oncogene product, but because of its antiapoptotic role,[3] it is utilized by tumor cells for survival.[4] Consequently, CK2 emerged as an attractive pharmacological target and plenty of chemically diverse ATP-competitive inhibitors have been developed.[5]

To avoid undesirable cross-reactivities with off-target kinases, several "jumping-out-of-the-catalytic-box" strategies of pharmacological intervention were suggested for CK2.[6] The most promising one takes advantage of the enzyme's intersubunit dynamics.[7] Perturbating the prominent CK2α/CK2β interaction[1] with artifical compounds might suppress specific CK2 holoenzyme functions like an increased stability[8] and an altered substrate specificity in comparison to unbound CK2α[9] resulting potentially in severe consequences on the CK2-related phosphoproteome.

This vision was supported by the discovery of a small molecule binding cavity located at CK2α's CK2β interface.[10] Laudet and co-workers applied a structure-based design approach[11] and a random screening strategy[12] to identify CK2β-competitive lead compounds. One of them is *Pc*: a cyclo peptide of the sequence GCRLYGFKIHGCG mimicking CK2β's C-terminal CK2α-interaction region. *Pc* interfers with the CK2α/CK2β complex formation, promotes the CK2α/CK2β dissociation, and was shown to disturb the CK2-holoenzyme-catalyzed phosphorylation of a CK2β-dependent CK2-substrate protein.[11]

A future optimization of *Pc* toward a peptidomimetic drug will benefit from a three-dimensional CK2α/*Pc* complex structure, from the thermodynamic profile of *Pc*'s affinity to CK2α and from the quantification of its impact on the CK2α/CK2β interaction. We provide these data here, supplemented by an investigation of *Pc*'s allosteric effect on the CK2α catalytic activity.

Initially, we validated the reported[11] competition between CK2β and *Pc* via an interaction assay based on *Escherichia coli* cell surface display.[13] A linear (noncyclized) variant of *Pc* with inverse amino acid sequence described to be devoid of any CK2β-competitive impact[11] served as a negative control molecule and is called "control peptide" hereafter.

CK2β^{1-193}, a C-terminally truncated CK2β-construct that is fully capable of interacting with CK2α,[14] was labeled by

Received: December 21, 2012
Accepted: March 8, 2013
Published: March 8, 2013

   dx.doi.org/10.1021/cb3007133 | *ACS Chem. Biol.* 2013, 8, 901–907

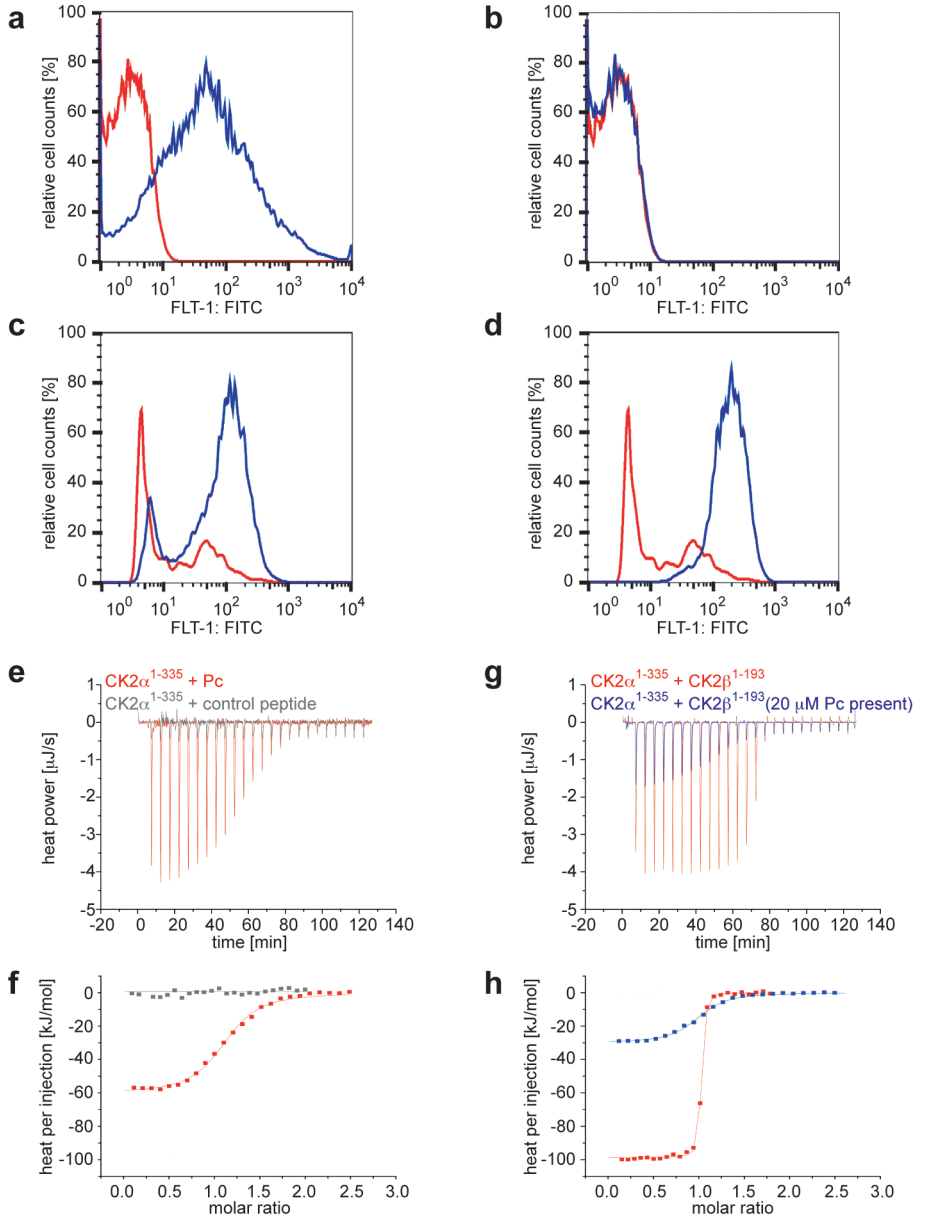

i

	$CK2\alpha^{1-335}$ + $CK2\beta^{1-193}$	$CK2\alpha^{1-335}$ + Pc	$CK2\alpha^{1-335}$ + $CK2\beta^{1-193}$ with presence of 20 µM Pc
K_D [nM]	4.03 ± 1.22	559.67 ± 256.70	239.92 ± 32.25
ΔG° [J/mol]	-49599 ± 743	-37056 ± 1047	-39068 ± 349
ΔH° [J/mol]	-94750 ± 4100	-56467 ± 3568	-30529 ± 1300
ΔS° [J/(mol*K)]	-146.65 ± 14.05	-60.85 ± 12.23	27.63 ± 3.62
stoichiometry	1.01 ± 0.01	1.03 ± 0.08	0.96 ± 0.06

Figure 1. Competitive CK2α/CK2β interaction analyses. (a–d) Autodisplay/flow cytometry assay using *E. coli* cells displaying CK2α (blue curves) or a control protein of similar size (red curves) after incubation with 0.77 μM FITC-labeled $CK2\beta^{1-193}$. (a,b) The blue curves illustrate the impact of $CK2\beta^{1-193}$-FITC without (a) and with (b) 10 min preincubation of the cells by 11.5 mM *Pc*. (c,d) Control experiments for (a,b) without (c) and with (d) 10 min preincubation of the cells by 11.5 mM control peptide. (e–i) Isothermal titration calorimetry (ITC) experiments: direct heat generation upon injection (e,g), and integrated and normalized heat data plus curve fits (f,h). (e,f) Analysis of the binding of *Pc* to $CK2\alpha^{1-335}$ (red) in comparison to the control peptide (gray). (g,h) Analysis of the $CK2\alpha^{1-335}$/$CK2\beta^{1-193}$ interaction in the absence (red) and in the presence of 20 μM *Pc* (blue). (i) Thermodynamic data (averages of at least three repetitions) from panels e–h. Second column, $CK2\beta^{1-193}$ injected to $CK2\alpha^{1-335}$; third column, *Pc* injected to $CK2\alpha^{1-335}$; fourth column, $CK2\beta^{1-193}$ injected to $CK2\alpha^{1-335}$ in the presence of 20 μM *Pc*.

fluorescein isothiocyanate (FITC) and then applied to *E. coli* cells displaying CK2α on their surface. As measured by flow cytometry, this resulted in a 68-fold increase in mean fluorescence in comparison to untreated control cells (Figure

dx.doi.org/10.1021/cb3007133 | *ACS Chem. Biol.* 2013, 8, 901–907

1a), indicating the specific binding of the CK2β^{1-193}–FITC adduct to surface-displayed CK2α. CK2β^{1-193}–FITC could even boost the mean fluorescence if the CK2α-displaying cells had been previously saturated with unlabeled CK2β^{1-193}, i.e., if unlabeled CK2β^{1-193} had to be replaced from its CK2α binding partner on the cell surface (Supplementary Figure 1). Finally, when cells displaying CK2α were preincubated for 10 min with 11.5 mM *Pc*, the increase in fluorescence after the addition of CK2β^{1-193}–FITC was completely suppressed (Figure 1b), indicating the CK2β-competitive potential of *Pc*. In contrast, 11.5 mM of the control peptide did not show any significant CK2β-competitive effect (Figure 1c,d).

Then, we co-crystallized *Pc* with CK2α^{1-335}, a C-terminal deletion mutant of human CK2α being catalytically active[15] and competent to bind CK2β.[14] The resulting CK2α^{1-335}/*Pc* complex crystals diffracted to 2.2 Å resolution (Table 1).

Table 1. Crystallographic Data Statistics

	CK2α^{1-335}/*Pc* complex
data collection	
temperature [K]	100
wavelength [Å]	1.0000
space group	$P2_12_12_1$
cell dimensions *a*, *b*, *c* [Å]	77.38, 105.42, 152.11
resolution range [Å]	45.69–2.20 (2.25–2.20)[a]
R_{sym}[b] [%]	6.2 (70.0)[a]
signal-to-noise ratio (I/σ_I)	21.75 (2.54)[a]
no. of unique reflections	63978 (6149)
multiplicity (measured/unique refl.)	6.55 (5.62)
completeness [%]	99.58 (95.89)[a]
Wilson B-factor [Å^2]	39.09
refinement	
resolution [Å]	45.69 – 2.20
no. of reflections in working set/test set	60187/3185
R_{work}/R_{free}	17.68/21.83
no. of atoms	
protein/cyclic peptide	8468/388
glycerol/chloride	54/3
water	462
r.m.s deviations	
bond lengths [Å]	0.004
bond angles [deg]	0.98
Ramachandran plot quality[b] [%]	
in favored regions	95.20
in allowed regions	4.32
outliers	0.48

[a]Values in parentheses are for highest resolution shell. [b]According to PHENIX.[24]

Their asymmetric unit contains three independent CK2α^{1-335} chains (A, B, and C) and four *Pc* peptides (chains D, E, F, and G; sequence numbering according to human CK2β; Figure 2a).

Each CK2α^{1-335} subunit binds one *Pc* peptide via the known[1] CK2β-binding site at the outer surface of the N-terminal β-sheet. The $\beta4/\beta5$-loop, an adaptable element of this region,[15] adopts its open, CK2-holoenzyme-similar conformation being untypical for unbound human CK2α (Figure 2a). *Pc* chain D, attached to CK2α^{1-335} subunit A, has the best defined electron density among these three *Pc* peptides. Therefore, the CK2α/*Pc* binding details are subsequently discussed on the basis of the couple CK2α^{1-335}-chain A/*Pc*-chain D.

The original design[11] implicated a high structural coincidence between the CK2α-bound forms of *Pc* and CK2β. In fact, the main chain RMS deviation for *Pc*/CK2β residues Arg186 to His193, i.e., for the central stretch of *Pc* being identical in sequence to CK2β is 1.06 Å on average, calculated after superimposition of the four N-lobal CK2α domains of the available CK2 holoenzyme structures (1JWH[1] and 4DGL[16]) on the equivalent region of CK2α^{1-335}-chain A. Thus, in contact to CK2α *Pc* adopts the same type-I β-hairpin loop motif as the equivalent CK2β region.[1] In this conformation, *Pc*'s backbone is intramolecularly stabilized by β-sheet-like hydrogen bonds. Moreover, the β-sheet enables direct and water-mediated main chain/main chain hydrogen bonds to CK2α (Figure 2b).

Concerning the side chains, *Pc* fits better to 4DGL[16] than to the lower resolved CK2 holoenzyme structure 1JWH.[1] Like in 4DGL, Phe190, CK2β's most important hot spot residue for the CK2α/CK2β interaction,[11] plunges deeply into a hydrophobic cavity of CK2α (Figure 2b) and touches Leu41, a hot spot on the CK2α-side of the CK2α/CK2β interaction.[17]

Alanine scanning along the *Pc* sequence had revealed[11] that, with decreasing priority, Gly189, Ile192, and Tyr188 are further crucial residues for the *Pc*/CK2α affinity. The Ile192 side chain does not directly contact CK2α (Figure 2c), but indirectly, it may contribute to the affinity via its inherent β-strand-stabilizing character.[18] Ile192, namely, is a member of *Pc*'s C-terminal β-strand, and as such, it forms main chain/main chain hydrogen bonds that stabilize the β-sheet conformation intramolecularly, couple it to strand $\beta1$ of CK2α, and extend it in this way into CK2α (Figure 2c).

Substituting Gly189 to alanine disturbs the *Pc*/CK2α interaction nearly as effectively as the removal of the Phe190 side chain.[11] In fact, the rather close contact of Gly189 to Asp103 from the $\beta4/\beta5$-loop of CK2α prohibits any side chain at this position (not shown). The whole spatially ambituous arrangement at the tip of *Pc*'s β-hairpin is a prerequisite for the establishment of a hydrogen-bonding network around CK2α's side chain Gln36. Several well-defined water molecules are part of this network (Figure 2c) and provide valuable hints for future attempts to derivatize *Pc* in order to optimize its affinity to CK2α.

Noteworthy, such water molecules are not visible in either of the CK2 holoenzyme structures.[1,16] The reason is probably not their genuine absence but the low resolutions of those structures (≥3 Å) since the space and hydrogen bonding partners required to accommodate water molecules are available in the CK2 holoenzyme as well. The generation of a water-assisted hydrogen-bonding pattern along the CK2α/CK2β assembly would correlate with its puzzling exothermic character, which was reported[14] (and reproduced in Figure 1g,h, red curves) but never satisfyingly explained. Most likely, water molecules fill H-bonding positions otherwise not saturated, which supplements the CK2α/CK2β interaction and emphasizes its nonoptimal and transient character[1,7] (and simultaneously the chances to interfere with it).

Finally, Tyr188 is only moderately important for the CK2α/*Pc* and the CK2α/CK2β interactions.[11] Consistently, in the CK2α^{1-335}/*Pc* structure, the backbone of Tyr188 is integrated in the aforementioned H-bonding network (Figure 2c), while its side chain is only loosely packed against Ile69 of CK2α. The OH-group of Tyr188 is in 2.9 Å distance to the terminal amino group of Lys71 (Figure 2d). This contact requires a particular Lys71 orientation enabled by a *cis*-configuration of the Lys71–Pro72 peptide bond (Figure 2d). Lys71 belongs to the strand

dx.doi.org/10.1021/cb3007133 | ACS Chem. Biol. 2013, 8, 901–907

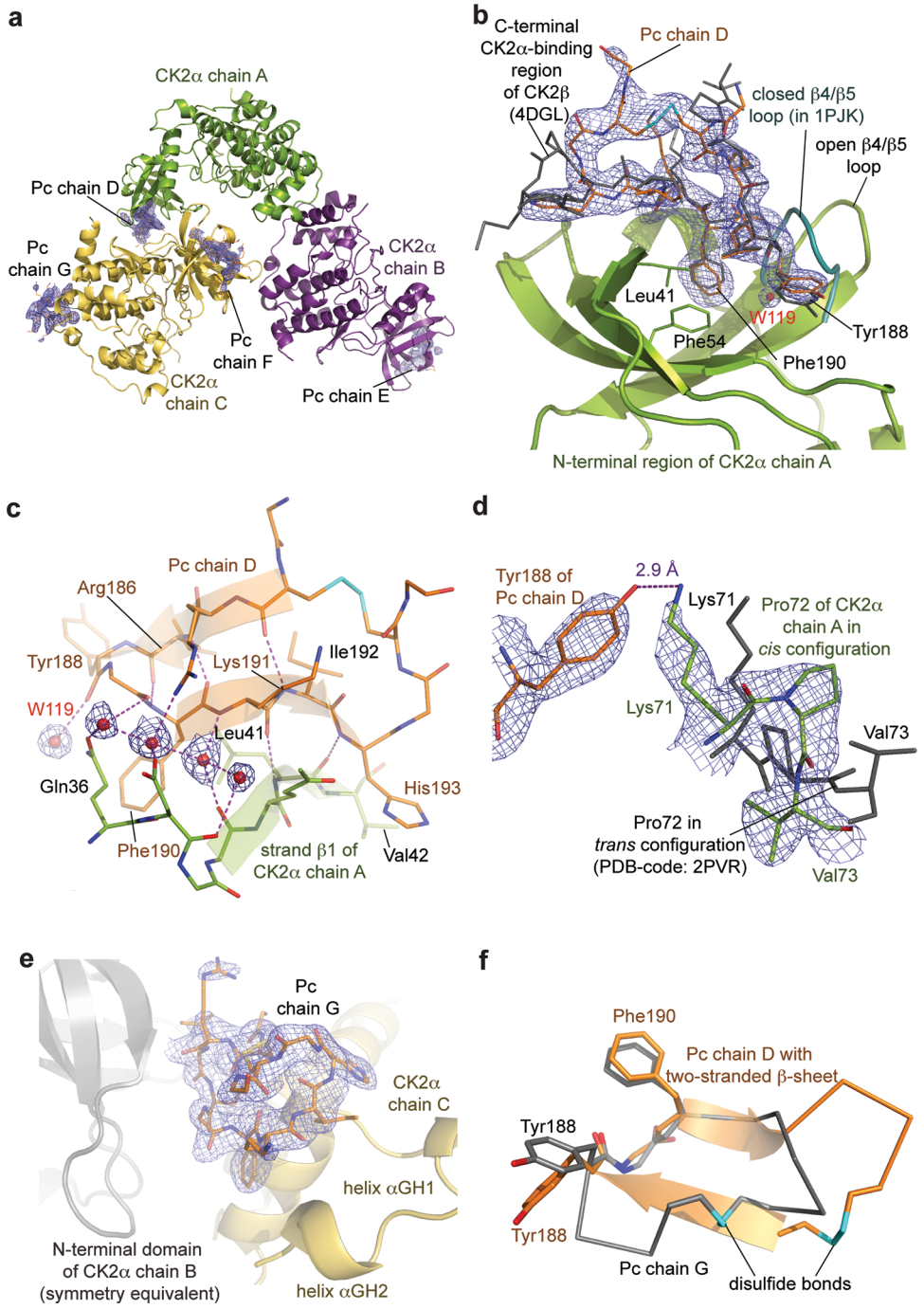

Figure 2. CK2α^{1-335}/*Pc* complex structure. (a) Overview of the asymmetric unit with three CK2α^{1-335} chains (green, magenta, and yellow) and four *Pc* molecules embedded in electron density. (b) *Pc* chain D and the buried water molecule W119 (both in electron density) at the CK2β interface of CK2α chain A (green). For comparison, a CK2β section from CK2 holoenzyme structure 4DGL[16] (black) and the closed β4/β5 loop from CK2α^{1-335} structure 1PJK[15] (blue) were drawn after superimposition of the corresponding CK2α chains. (c) Extension of CK2α's N-lobal antiparallel β-sheet into bound *Pc* peptide assisted by water-mediated hydrogen bonds. (d) Cis-configuration of the Lys71/Pro72 pepide bond within the β3/αC-loop of CK2α^{1-335} enabling the approximation of the Lys71 side chain to the *Pc* peptide. Black: Lys71−Val73 stretch with *trans*-Pro72 from CK2α^{1-335} structure 2PVR. (e) Binding site of *Pc* chain G by the C-lobe of CK2α^{1-335} chain C and the N-lobe of CK2α^{1-335} chain B. (f) Conformational flexibility of *Pc* revealed by superimposition of the Tyr188/Gly189/Phe190-tripeptides of *Pc* molecules D (orange C-atoms) and G (black C-atoms). The figure was prepared with PyMOL (Schrödinger, LLC.). Electron density pieces were contoured at 1.0 σ. Red dotted lines indicate hydrogen bonds.

β3/helix αC loop connection, which is rather short in CK2α since it misses the helix αB of the canonical protein kinase fold. No significant plasticity of CK2α's β3/αC loop and, in particular, no *cis*-configuration at Pro72 was described before. Such a native state proline isomerization[19] without a specific *cis*/*trans* isomerase is a rare, but known phenomenon. It can serve as a molecular switch, but whether it is functionally important in CK2α remains open at the moment.

If a small, conformationally flexible molecule is coordinated at a protein surface, an entropic penalty is unavoidable.

dx.doi.org/10.1021/cb3007133 | *ACS Chem. Biol.* 2013, 8, 901−907

Therefore, *Pc* intentionally contains a disulfide bond for cyclization.[11] Nevertheless, *Pc*, unlike CK2β itself where the critical β-hairpin motif is preformed,[14] still requires conformational adaption during CK2α-binding.

Accidentally, the CK2α^{1-335}/*Pc* structure reveals this by a fourth *Pc* peptide (chain G) providing a second conformational snapshot. *Pc*−G is unspecifically intercalated between two CK2α^{1-335} subunits (Figure 2e). The Tyr188−Gly189−Phe190 motif of *Pc*−G is similar to *Pc*−D but the rest of the molecule largely deviates (Figure 2f). In particular, no β-hairpin structure is formed (Figure 2f). Consequently, a synthetic stabilization of *Pc*'s β-hairpin conformation should further reduce the enthalpic loss upon CK2β-competitive binding to CK2α and thus improve the *Pc*/CK2α affinity.

We revealed via ITC that *Pc* binds significantly more weakly to CK2α^{1-335} than CK2β^{1-193}, while the control peptide shows no indications of any affinity to CK2α^{1-335} (gray curves in Figure 1e,f). The determined K_D value of 559.7 nM (red curves in Figure 1e,f,i) [compared to 4.0 nM for the CK2α^{1-335}/CK2β^{1-193} interaction (red curves in Figure 1g,h,i)] is a type of K_I value with respect to the CK2α/CK2β interaction; qualitatively, it fits to the IC_{50} value of 3 μM, reported for *Pc*'s impact on the CK2α/CK2β assembly.[11] A quantitative conversion of these data is impossible because that IC_{50} value had been determined with an immobilized CK2β construct.[11]

The higher affinity of CK2β^{1-193} suggests the existence of contact regions outside the β-hairpin motif *Pc* is mimicking. In fact, with about 510 Å^2, the CK2α^{1-335}/*Pc* interface is significantly smaller than the 830 Å^2 reported for the CK2α/CK2β interface in the CK2 holoenzyme[1] where especially the CK2β helix αF provides further contacts to CK2α.

Despite these differences, the thermodynamic signatures of *Pc* and CK2β^{1-193} concerning CK2α^{1-335} binding are similar. In both cases, the affinity is governed by a large enthalpic contribution that overcompensates an infavorable entropic term of significant height (red graphs in Figure 1e,f,g,h). This analogy is consistent with the common binding modes of *Pc* and CK2β. It shows that *Pc* can serve as a peptidic model of CK2β in approaches to screen for further competitors of the CK2α/CK2β interaction.

Then, we used ITC to quantify the CK2β-competitive potential of *Pc*, namely, by ITC titration of CK2β^{1-193} against CK2α^{1-335} in the presence of 20 μM *Pc* (blue curves in Figure 1g,h; final column of Figure 1i). In this case, CK2β^{1-193} first had to replace *Pc* to get access to its binding site on the CK2α^{1-335} surface, which required energy. Consequently, the heat development (and accordingly the interaction enthalpy) was significantly reduced compared to the *Pc*-free titration (red curves in Figure 1g,h; second column of Figure 1i).

Partly this loss of interaction enthalpy is compensated by entropy (Figure 1i), with −8514 J/mol, the entropic term ($-T^*\Delta S^\circ$) that supports the interaction presumably because the release of the *Pc* peptide enables its conformational flexibility. In summary, however, the affinity between CK2β^{1-193} and CK2α^{1-335} is reduced by *Pc* as reflected by an apparent dissociation constant $K_{D,app}$ of 239.9 nM compared to 4.0 nM in the absence of *Pc*. A calculation of $K_{D,app}$ according to $K_{D,app} = K_D[1 + c_{Pc}/K_I] = 4.0\ \text{nM}[1 + (20\ \mu\text{M})/(559.7\ \text{nM})]$ leads to 147 nM, which is coarsly in the same range.

How does *Pc* effect the catalytic activity of CK2? The answer to this question critically depends on the nature of the catalyst, CK2 holoenzyme or unbound CK2α, and of the substrate.[9] Using the CK2 holoenzyme and a so-called class-III substrate,[9] i.e., a protein that critically requires an intact CK2α/CK2β assembly for phosphorylation, Laudet et al.[11] showed that the catalytic activity was efficiently disturbed by *Pc*.

To supplement this result, we tested the effect of *Pc* on the catalytic activity of unbound CK2α with a substrate peptide rather than a protein. We observed a stimulatory effect of *Pc* on CK2α^{1-335} (Figure 3a) similar to that of CK2β (Figure 3c), yet

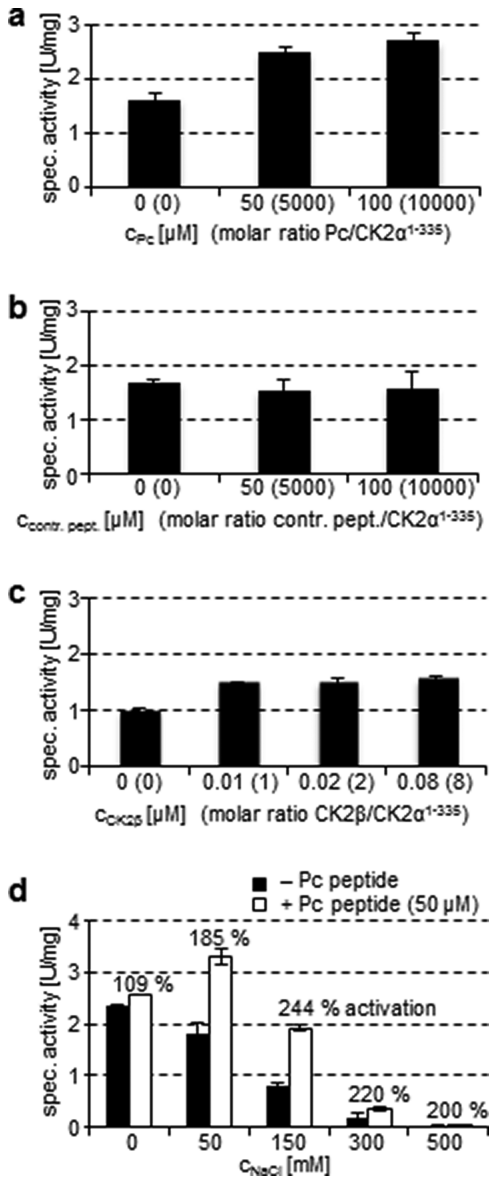

Figure 3. Catalytic activity test. (a−c) Impact of the *Pc* peptide (a) and for comparison the control peptide (b) and CK2β (c) on the enzymatic activity of CK2α^{1-335}. (d) Partial protection of CK2α^{1-335} activity by *Pc* against salt inactivation. The percentage of activation by *Pc* is given for each NaCl concentration. The bars represent average values from triplicate measurements. Standard deviations are indicated.

with a significantly higher molar ratio required to achieve saturation. For comparison, the control peptide did not show any up- or downregulation of the catalytic activity (Figure 3b) consistent with its inability to bind to CK2α^{1-335} (Figure 1e,f).

The stimulatory effect of *Pc* on CK2α^{1-335} was also visible when we investigated the catalytic activity of CK2α as a function of the NaCl concentration. The background of this experiment was the observation of Grankowski et al.[20] that the

dx.doi.org/10.1021/cb3007133 | ACS Chem. Biol. 2013, 8, 901−907

activity of CK2α strongly decreases with increasing KCl concentrations. Here, we found a similar inhibitory effect of NaCl (Figure 3d). In the presence of 50 μM *Pc*, however, this inactivation is attenuated (Figure 3d) revealing a mean stimulation factor of 1.92 and a protective impact of *Pc* on CK2α that resembles that of CK2β.

Thus, *Pc* is an allosteric activator of CK2α, to our knowledge the first one to be described except for CK2β.

METHODS

Expression and Purification of Proteins. Human CK2α^{1-335}, CK2β^{1-193}, and wild-type CK2β were expressed and purified as described elsewhere.[14,20] The purified proteins were concentrated and rebuffered in 500 mM NaCl and 25 mM Tris/HCl, pH 8.5, by ultrafiltration.

Peptide Synthesis. *Pc* and its linear variant with inversed sequence were prepared using solid phase synthesis based on Wang resin with an automated robot following the Fmoc/*t*-Bu strategy. The completed peptides were cleaved from the resin with trifluoroacetic acid (TFA) plus scavengers (TFA/H_2O/ethanedithiol/triisopropylsilane, 94/2.5/2.5/1), precipitated in ether and purified by preparative HPLC. To generate *Pc*, the peptide was dissolved in 10 mM NH_4HCO_3, pH 8, and cyclized by air oxidation with the addition of H_2O_2. After 45 min, the reaction was stopped by adding TFA. The crude mixture was purified by size exclusion chromatography using an SPE-column (Chromafix). The eluate was lyophilized and analyzed by LC-ESI-MS (LCQ, finniganMAT, Thermo). *Pc*, 1408.68 g/mol; ESI-MS, 1408.91 $[M + H]^+$, 705.22 $[M + 2H]^{2+}$, 470.45 $[M + 3H]^{3+}$.

Autodisplay Competition Assay. FITC was coupled to CK2β^{1-193} using a kit from Calbiochem. *E. coli* BL21(DE3) cells genetically prepared to display CK2α[13] were grown to the mid log phase (OD_{600} = 0.5), harvested, and suspended in the same volume of phosphate-buffered saline solution (PBS). Protein expression was induced by adding 1 mM IPTG (final concentration) for 16 h at 30 °C. Subsequently, cells were washed three times and suspended in PBS to an OD_{600} = 0.35. CK2β^{1-193}–FITC was added in a final concentration of 0.77 μM for 1 h in the dark either without or with preincubation with 11.5 mM *Pc* or the control peptide for 10 min in the dark. Cells were washed three times with filter sterilized PBS and suspended in 50 μL of filter sterilized PBS containing 0.1% Tween. Fluorescence was measured with a FACSCalibur (BD, Heidelberg, Germany), using 488 nm as excitation wavelength, 530 nm for detection, and filter-sterilized PBS as sheath fluid as described before.[21] Solely intact cells were analyzed after background noise elimination. For each sample, at least 50,000 events were counted using a flow rate of 1000 events per s.

Structure Determination. CK2α^{1-335}/*Pc* cocrystals were obtained by vapor diffusion using the "JBScreen-Classic HTS I" crystallization screen from JenaBioscience. The optimized crystallization drop contained 0.5 μL of CK2α^{1-335} (12 mg mL^{-1}) + 0.3 μL of 5 mM *Pc* + 0.2 μL of 500 mM NaCl, 25 mM Tris/HCl, pH 8.5 + 1 μL of reservoir solution, which was composed of 9% (w/v) PEG 8000 and 100 mM Tris/HCl, pH 8.5. Crystals appeared after 3–4 weeks. Cryo conditions were achieved with 10% (v/v) glycerol, 30% (w/v) PEG 8000, and 100 mM Tris/HCl, pH 8.5.

X-ray diffraction data were collected at the Swiss Light Source, Villigen, using a wavelength of 1 Å and a temperature of 100 K. The diffration data were processed with XDS.[22] The structure was solved by molecular replacement using PHASER[23] and refined with PHENIX.[24] Manual corrections were performed with COOT.[25] The final structure is available from the PDB under code 4IB5.

Isothermal Titration Calorimetry. All ITC experiments were performed with a Microcal VP-ITC at 35 °C. Protein concentrations where determined by absorbance at 280 nm. Peptide (*Pc* or control peptide) stock solutions with defined concentrations were prepared by weighting the solid powders. Both proteins and peptides were solved in 500 mM NaCl and 25 mM Tris/HCl, pH 8.5, to the required concentrations and subsequently degassed. CK2α^{1-335} (20 μM) was provided in the sample cell and was titrated with either CK2β^{1-193} or *Pc* (200 μM). Each ITC experiment consisted of one initial injection of 2 μL, followed by 24 injections of 10 μL. The injections were made over a period of 20 s with a 300 s interval between subsequent injections. The original heat production upon injection (Figure 1e,g) was integrated using the ORIGIN software (version 7, Origin Lab) and corrected by subtracting the corresponding heat of dilution. For curve fitting through the integrated, dilution corrected, and normalized peaks (Figure 1f,h), the "*single set of sites*" model was used.

Kinase Assays. CK2α^{1-335} was preincubated at RT for 10 min with *Pc* and NaCl in various concentrations. The final assay mix (50 μL) contained 0.5 pmol CK2α^{1-335}, 25 mM Tris/HCl, pH 8.5, 5 mM $MgCl_2$, 125 μM [γ-^{32}P]ATP, 100 μM synthetic peptide substrate (sequence RRRADDSDDDDD), and *Pc*, control peptide, or CK2β in concentrations given in Figure 3. The NaCl concentration was 150 mM for Figure 3a–c and variable for Figure 3d as indicated in the figure. The kinase reactions were run for 10 min at 30 °C and stopped by setting the samples on ice. Subsequently, 20 μL reaction mixtures were spotted onto P81 phosphocellulose paper (Whatman). Filter papers were extensively washed with 85 mM phosphoric acid. The amount of incorporated radioactivity was determined with a scintillation counter.

ASSOCIATED CONTENT

Supporting Information

Autodisplay assay to probe the competition between unlabeled CK2β^{1-193} and FITC-labeled CK2β1-193 for binding at surface-displayed CK2α. This material is available free of charge *via* the Internet at http://pubs.acs.org.

AUTHOR INFORMATION

Corresponding Author

*E-mail: Karsten.Niefind@uni-koeln.de.

Notes

The authors declare no competing financial interests.

ACKNOWLEDGMENTS

We are grateful to S. Waltersperger for diffraction data collection at the SLS, to K. Splith, F. Reichart, A. Gill, and E. Yoo for peptide synthesis, and to Tine D. Rasmussen for excellent technical lab assistance. This work was funded by the Deutsche Forschungsgemeinschaft (grant: NI 643/4-1).

REFERENCES

(1) Niefind, K., Guerra, B., Ermakowa, I., and Issinger, O.-G. (2001) Crystal structure of human protein kinase CK2: insights into basic properties of the CK2 holoenzyme. *EMBO J. 20*, 5320–5331.

(2) Guerra, B., and Issinger, O.-G. (2008) Protein kinase CK2 in human diseases. *Curr. Med. Chem. 15*, 1870–1886.

(3) Ahmed, K., Gerber, D. A., and Cochet, C. (2002) Joining the cell survival squad: an emerging role for protein kinase CK2. *Trends Cell Biol. 12*, 226–230.

(4) Ruzzene, M., and Pinna, L. A. (2010) Addiction to protein kinase CK2: A common denominator of diverse cancer cells? *Biochim. Biophys. Acta, Proteins Proteomics 1804*, 499–504.

(5) Cozza, G., Meggio, F., and Moro, S. (2011) The dark side of protein kinase CK2 inhibition. *Curr. Med. Chem. 18*, 2867–2884.

(6) Prudent, R., and Cochet, C. (2009) New protein kinase CK2 inhibitors: jumping out of the catalytic box. *Chem. Biol. 16*, 112–120.

(7) Filhol, O., Nueda, A., Martel, V. V., Gerber-Scokaert, D., Benitez, M. J., Souchier, C., Saoudi, Y., and Cochet, C. (2003) Live-cell fluorescence imaging reveals the dynamics of protein kinase CK2 individual subunits. *Mol. Cell. Biol. 23*, 975–987.

(8) Boldyreff, B., Meggio, F., Pinna, L. A., and Issinger, O.-G. (1993) Reconstitution of normal and hyperactivated forms of casein kinase-2 by variably mutated β-subunits. *Biochemistry 32*, 12672–12677.

(9) Pinna, L. A. (2002) Protein kinase CK2: a challenge to canons. *J. Cell Sci. 115*, 3873−3878.
(10) Raaf, J., Brunstein, E., Issinger, O.-G., and Niefind, K. (2008) The CK2α/CK2β interface of human protein kinase CK2 harbors a binding pocket for small molecules. *Chem. Biol. 15*, 111−117.
(11) Laudet, B., Barette, C., Dulery, V., Renaudet, O., Dumy, P., Metz, A., Prudent, R., Deshiere, A., Dideberg, O., Filhol, O., and Cochet, C. (2007) Structure-based design of small peptide inhibitors of protein kinase CK2 subunit interaction. *Biochem. J. 408*, 363−373.
(12) Laudet, B., Moucadel, V., Prudent, R., Filhol, O., Wong, Y.-S., Royer, D., and Cochet, C. (2008) Identification of chemical inhibitors of protein-kinase CK2 subunit interaction. *Mol. Cell. Biochem. 316*, 63−69.
(13) Jose, J., Maas, R. M., and Teese, M. G. (2012) Autodisplay of enzymes: molecular basis and perspectives. *J. Biotechnol. 161*, 92−103.
(14) Raaf, J., Brunstein, E., Issinger, O.-G., and Niefind, K. (2008) The interaction of CK2α and CK2β, the subunits of protein kinase CK2, requires CK2β in a preformed conformation and is enthalpically driven. *Protein Sci. 17*, 2180−2186.
(15) Ermakova, I., Boldyreff, B., Issinger, O.-G., and Niefind, K. (2003) Crystal structure of a C-terminal deletion mutant of human protein kinase CK2 catalytic subunit. *J. Mol. Biol. 330*, 925−934.
(16) Lolli, G., Pinna, L. A., and Battistutta, R. (2012) Structural determinants of protein kinase CK2 regulation by autoinhibitory polymerization. *ACS Chem. Biol. 7*, 1158−1163.
(17) Raaf, J., Bischoff, N., Klopffleisch, K., Brunstein, E., Olsen, B. B., Vilk, G., Litchfield, D. W., Issinger, O.-G., and Niefind, K. (2011) Interaction between CK2α and CK2β, the subunits of protein kinase CK2: thermodynamic contributions of key residues on the CK2α surface. *Biochemistry 50*, 512−522.
(18) Swindells, M. B., MacArthur, M. W., and Thornton, J. M. (1995) Intrinsic ϕ,ψ propensities of amino acids, derived from the coil regions of known structures. *Nat. Struct. Biol. 2*, 596−603.
(19) Andreotti, A. H. (2003) Native state proline isomerization: an intrinsic molecular switch. *Biochemistry 42*, 9515−9524.
(20) Grankowski, N., Boldyreff, B., and Issinger, O.-G. (1991) Isolation and characterization of recombinant human casein kinase II subunits α and β from bacteria. *Eur. J. Biochem. 198*, 25−30.
(21) Jose, J., Betscheider, D., and Zangen, D. (2005) Bacterial Surface Display Library Screening by target enzyme labelling: Identification of new human cathepsin G inhibitors. *Anal. Biochem. 346*, 258−267.
(22) Kabsch, W. (2010) XDS. *Acta Crystallogr. D66*, 125−132.
(23) McCoy, A. J., Grosse-Kunstleve, R. W., Adams, P. D., Winn, M. D., Storoni, L. C., and Read, R. J. (2007) Phaser crystallographic software. *J. Appl. Crystallogr. 40*, 658−674.
(24) Adams, P. D., Afonine, P. V., Bunkóczi, G., Chen, V. B., Davis, I. W., Echols, N., Headd, J. J., Hung, L.-W., Kapral, G. J., Grosse-Kunstleve, R. W., McCoy, A. J., Moriarty, N. W., Oeffner, R., Read, R. J., Richardson, D. C., Richardson, J. S., Terwilliger, T. C., and Zwart, P. H. (2010) PHENIX: a comprehensive Python-based system for macromolecular structure solution. *Acta Crystallogr. D66*, 213−321.
(25) Emsley, P., Lohkamp, B., Scott, W. G., and Cowtan, K. (2010) Features and development of Coot. *Acta Crystallogr. D66*, 486−501.